Computational Materials Science 171 (2020) 109226

Contents lists available at ScienceDirect

Computational Materials Science

journal homepage: www.elsevier.com/locate/commatsci

First-principles investigation of monatomic gold wires under tension

Lianhua He[a], Fang Liu[b], Ju Li[c], Gian-Marco Rignanese[d,*], Aihui Zhou[e,f]

[a] Department of High Performance Computing Technology and Application Development, Computer Network Information Center, Chinese Academy of Sciences, Beijing 100190, China
[b] School of Statistics and Mathematics, Central University of Finance and Economics, Beijing 100081, China
[c] Department of Nuclear Science and Engineering and Department of Materials Science and Engineering, Massachusetts Institute of Technology, Cambridge, MA 02139, USA
[d] European Theoretical Spectroscopy Facility (ETSF) and Institute of Condensed Matter and Nanosciences (IMCN), Université Catholique de Louvain, Chemin des Étoiles 8, 1348 Louvain-la-Neuve, Belgium
[e] LSEC, Institute of Computational Mathematics and Scientific/Engineering Computing, Academy of Mathematics and Systems Science, Chinese Academy of Sciences, Beijing 100190, China
[f] School of Mathematical Sciences, University of Chinese Academy of Sciences, Beijing 100049, China

ARTICLE INFO

Keywords:
First-principles calculations
Gold nanowires
Phonons
Kohn anomalies
Peierls instability

ABSTRACT

Ab initio pseudopotential total-energy calculations on infinite monatomic chains of Au are performed within density functional theory. We use the density functional perturbation theory to study the phonon spectra of these gold wires as a function of strain. Our results show that there does not seem to be a range of strain for which the linear chain is stable, contrary to what was stated by Ribeiro and Cohen [Phys. Rev. B 68 (2003) 035423]. For low strain, the zigzag chain is the stable geometry; while for higher strain, the chains with two or more aligned gold atoms are found to be more stable. At the limit between these two regimes, we predict a transition structure (an asymmetric zigzag chain) to be the most stable.

1. Introduction

Metallic nanocontacts have been the subject of many recent investigations. Among these, gold nanowires have attracted considerable attention. Indeed, they display very interesting properties from a basic science standpoint but also have many potential applications (e.g, in nanoelectronics). In particular, gold nanowires have the ability to evolve into linear chains which present large Au-Au interatomic distances before breaking [1–3].

Many experimental works have been devoted to the characterization of the mechanical properties of gold nanowires [1,2,4–11]. The experimental Au-Au distance reported in the literature varies quite a lot depending on the production method and the measurement technique [1,5,6].

A great deal of theoretical research has also been dedicated to gold nanowires using density functional theory (DFT) [12–37]. Hereafter, we only mention the results obtained for monatomic nanowires. These adopt a zigzag shape which remains stable under tension and only become linear just before breaking [12], hence explaining the observed large interatomic distances. It was also argued that a linear monatomic gold wire should be unstable at atomic distances greater than about 3 Å and that it should dimerize [18,19]. These findings were further confirmed by an investigation of the equilibrium configurations of an infinite chain depending upon stretching and compressing [20].

Several works have also considered the stability of the monatomic gold chains by computing the phonon frequencies [12,14,15]. Using the frozen-phonon approximation, Ribeiro and Cohen [14] computed the phonon frequencies at the X point for the linear chain. They concluded that there is a range of strains (for a length per atom comprised between 2.71 and 2.83 Å) for which the linear wire is stable. Using density-functional perturbation theory (DFPT), Picaud et al. [15] arrived at the similar conclusion (the range of stability being comprised between 2.75 and 2.85 Å). The phonon frequencies of the zigzag wire were also investigated as functions of the length per atom (also using the frozen-phonon approximation) [12]. It was found that the phonon dispersion curve stays positive in the whole Brillouin zone for a length of 2.62 Å per atom. But the longitudinal mode becomes negative beyond 2.9 Å per atom, which was interpreted as a breaking of the wire.

Due to the importance of the monatomic gold nanowires, in this paper, we studied several gold wires with different structures under tension. The structural, energetic, and mechanical properties of these gold wires are computed. Especially the phonon instability for linear, zigzag, and dimer gold chains are studied by DFPT.

The paper is organized as follows. The methodological aspects of

* Corresponding author.
E-mail address: gian-marco.rignanese@uclouvain.be (G.-M. Rignanese).

https://doi.org/10.1016/j.commatsci.2019.109226
Received 29 April 2019; Received in revised form 16 August 2019; Accepted 26 August 2019
Available online 03 September 2019
0927-0256/

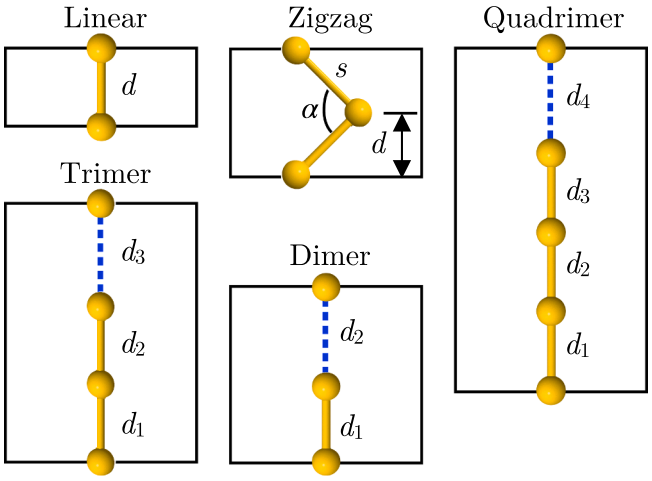

Fig. 1. Structures of the linear, zigzag, dimer, trimer and quadrimer chains.

our study are developed in Section 2. Then, our results are presented and discussed in Section 3. The possible structure and the energetics of the different chains are investigated (see 3.1). The stability is analyzed in more details by computing the phonon bandstructures (see 3.2). Finally, our findings are summarized in Section 4.

2. Methodology

All the calculations are performed using DFT [38] and DFPT [39,40], as implemented in the ABINIT [41] code. The exchange-correlation energy is evaluated within the local-density approximation (LDA) using the Perdew-Wang functional, which performs very well for vibrational properties of solids [42]. The interaction of the valence electrons with the ionic cores is represented with a separable, norm-conserving Troullier-Martins [43]. The wave functions are expanded into plane-waves up to a cutoff energy of 20 Ha (544 eV), which guarantees an accuracy of ~0.005 Å on the bond lengths and of ~0.5 cm^{-1} on the phonon frequencies.

We use a tetragonal periodic cell allowing for 20 Å vacuum between the wires. Different configurations of the chain are considered (see Fig. 1). The smallest unit cell with one atom per cell (referred to as linear chain) corresponds to the infinite monatomic chain. We also consider the double unit cell in order to allow for either a dimerization (see dimer chain in Fig. 1) or the formation of a zigzag (see zigzag chain in Fig. 1) along the chain. Finally, we consider other multiples (N-mer with $N = 3$, 4, 5, and 6) of the original cell (only the trimer and quadrimer are illustrated in Fig. 1).

The Brillouin Zone (BZ) integrations were performed within Monkhorst-Pack (MP) scheme. For the smallest unit cell, a $100 \times 1 \times 1$ k-point grid was used. For the larger unit cells, the k-point sampling was adapted to achieve a similar density in the BZ. The energy levels are populated using either a Gaussian broadening [44] or a Fermi-Dirac (FD) distribution within Mermin's generalization [45] of DFT to the canonical ensemble. The latter technique explicitly accounts for the effect of temperature. Unless otherwise stated, the results presented in the paper are obtained using a Gaussian smearing of 0.001 Ha (27.2 meV). With these parameters, the total-energy precision is better than 1 meV/atom.

The DFPT phonon calculations are limited to the linear, dimer, and zigzag chains. Special care must be taken due to the possible presence of both Kohn anomalies [46] and Peierls instabilities [47] as it will be discussed later on. Hence, we use both the usual interpolation techniques based on the explicit calculation of the dynamical matrices on regular q-point grids and a cubic spline interpolation of the phonon frequencies computed on a non-uniform grid of q-points.

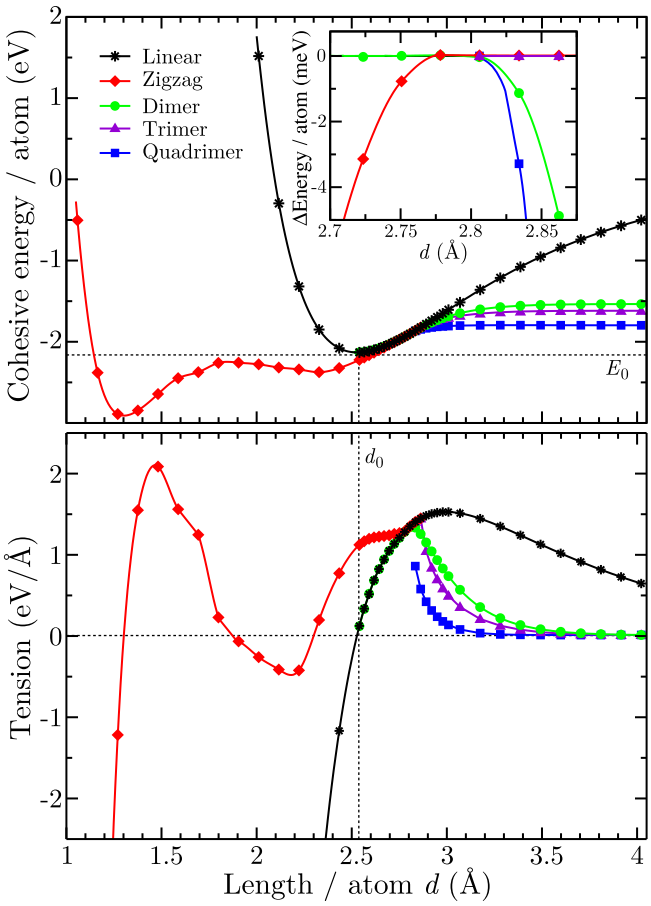

Fig. 2. Calculated cohesive energy per atom (calculated with respect to the isolated atom) and tension of Au chains as a function of the length per atom d.

3. Results and discussions

3.1. Structure and energetics

We first relax the geometry for the linear chain. We find that the equilibrium length per atom d_0 is 2.54 Å, which is in agreement with the experimental value 2.5 ± 0.2 Å [6]. This is also consistent with the previous theoretical values 2.56 Å[12,13] and 2.49 Å[14,15].

We also study the structural parameters, energetics, and mechanical properties of the linear, zigzag, dimer, trimer and quadrimer chains, which are illustrated in Fig. 1. The cohesive energy per atom E_{coh} (computed with respect to the isolated atom) and the tension are reported in Fig. 2 as a function of the length per atom for these five different structures. A given length per atom d can easily be converted into a strain ε with respect to the equilibrium length per atom for the linear chain d_0 by $\varepsilon = \frac{d}{d_0} - 1$.

Due to the well-known Peierls distortion [47], a uniform one-dimensional chain with a partially filled band cannot be stable. As can be seen in the upper panel of Fig. 2, the zigzag and dimer chains are indeed found to be energetically favored depending on the strain (the length per atom).

At very low and negative strain ($\varepsilon < 0.09$, $d < 2.78$ Å), the zigzag chain is the most stable. The corresponding energy (tension) curve actually shows two minima (zeroes) for a length per atom d of 1.27 and 2.31 Å ($\varepsilon = -0.50$ and -0.09). The angles α are calculated to be roughly 56° and 135° at these two energy minima. These are very similar to the theoretical results reported in Ref. [13] (60° and 131°) and Ref. [17] (58.8° and 130.6°). As we stretch the zigzag chain, the angle α increases monotonically up to 180° (linear chain), as can be seen in the upper panel of Fig. 3. Then, it becomes a linear chain (the red dots in

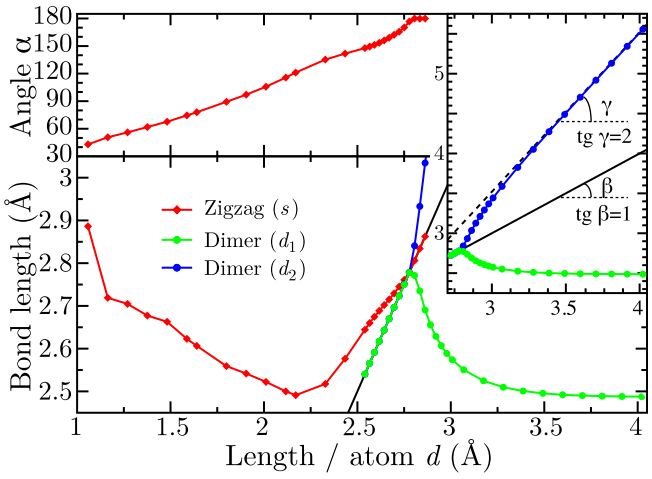

Fig. 3. Evolution of the structural parameters of the zigzag (s and α in Fig. 1) and and the dimer (d_1 and d_2) chain as a function of the length per atom. The angle α is reported in the upper panel, while the distances s, d_1, and d_2 are shown in the lower panel. The panel on the right focuses on the dimer chain showing the asymptotic behavior (when the bond is broken). The solid black line represents the linear chain. Its slope is equal to 1 (since the bond length is exactly the length per atom), whereas the slope of the dashed line is equal to 2.

the lower panel of Fig. 3 follow the black solid line).

At high strain ($\varepsilon > 0.10$, $d > 2.80$ Å), the dimerized chain is more stable than the linear one. Actually, before $d = 2.80$ Å, there is basically no dimerization (the green and blue dots in the lower panel of Fig. 3 follow the black solid line). Beyond, one of the bond lengths (d_1 in green) slowly converges towards the isolated dimer value 2.49 Å, while the second one (d_2 in blue) tends to be proportional to the lattice parameter, hence to twice the length per atom, as indicated by the black dashed in the right panel of Fig. 3.

In the upper panel of Fig. 2, we can see that the trimer and quadrimer chains are even more energetically favorable than the dimer: when the chain is stretched, one of the bonds in the wire breaks. This is in accordance with results of Ref. [17] in which the linear, dimer, and quadrimer gold chains were studied. In fact, as the number of atoms N in the unit cell increases, the corresponding cohesive energy per atom $E_{\mathrm{coh}}(N)$ decreases. This can also be seen in Table 1 where we report the asymptotic value (as length per atom goes to infinity, the energy does not change anymore upon pulling the nanowire in the broken structure). In this Table, we also indicate the values calculated for a pentamer ($N = 5$) and an hexamer ($N = 6$). Note that in these latter cases, we did not compute the full energy curve but just the asymptotic value (which is obtained by allocating a distance larger than 5 Å to the broken bond). From the upper panel of Fig. 2 and Table 1, it seems that $E_{\mathrm{coh}}(N)$ decreases towards the equilibrium energy of the linear gold chain ($E_0 = -2.131$ eV/atom) as the number of atoms N increases. Indeed, as

Table 1
Asymptotic values of the cohesive energy per atom (E_{coh}), the energy of broken bond (E_{BB}), the different nearest-neighbor distances as a function of the number of atoms N in the unit cell.

	$N = 2$	$N = 3$	$N = 4$	$N = 5$	$N = 6$
Energies (in eV)					
E_{coh}	−1.536	−1.619	−1.797	−1.839	−1.896
E_{BB}	1.189	1.536	1.335	1.457	1.405
Distances (in Å)					
d_1	2.49	2.52	2.51	2.51	2.51
d_2		2.52	2.58	2.53	2.58
d_3			2.51	2.53	2.54
d_4				2.51	2.58
d_5					2.51

N goes to infinity the system goes closer and closer to the perfect linear chain plus a broken bond. This is also confirmed by the asymptotic geometry of the different structure (see distances in Table 1). The bonds inside the chain quickly approach the equilibrium value $d_0 = 2.54$ Å. Finally, we compute the energy of the broken bond (E_{BB}) as the difference between the cohesive energy of the equilibrium geometry for the linear chain and the asymptotic cohesive energy $E_{\mathrm{coh}}(N)$ for a given N-mer (with a completely broken wire): $E_{\mathrm{BB}} = E_{\mathrm{coh}}(N) - NE_0$. The calculated values of E_{BB} are reported in Table 1 for different structures. As N increases, E_{BB} converges towards 1.4–1.5 eV. This value is significantly bigger than the value 0.87 eV reported in Ref. [17], that was calculated using the GGA for the exchange-correlation and limited to the case of the quadrimer (that is slightly lower than for the pentamer and hexamer).

The inset of the upper panel of Fig. 2 focuses on the transition from the region where the zigzag chain is the most stable to the region where it is the dimer chain. The difference in energy with respect to the linear chain is reported for $d = 2.72$, 2.75, 2.78, 2.81, 2.83, and 2.86 Å ($\varepsilon = 0.07$, 0.08, 0.09, 0.10, 0.11, and 0.12). For the two central points ($d = 2.78$ Å, $\varepsilon = 0.09$ and $d = 2.81$ Å, $\varepsilon = 0.10$), the difference in energy between the linear, zigzag, and dimer chain falls below 1 meV (reaching the limit of the accuracy of our total energy calculations). For these values of the strain, calculations of the phonon bandstructures are highly desirable. For $d < 2.78$ Å ($\varepsilon < 0.09$), the dimer chain is strictly equivalent to the linear chain; and similarly, for $d > 2.81$ Å ($\varepsilon > 0.10$), the same happens for the zigzag chain. For those values of the length per atom (strain), the trimer chain (purple curve with triangles) is also equivalent to the linear chain. There is not enough room for a bond to break. For $d = 2.83$ Å ($\varepsilon = 0.11$), the quadrimer (blue curve with squares) is already more stable than the dimer. But, it was not possible to stabilize it for $d = 2.81$ Å ($\varepsilon = 0.10$): whatever the starting point, the system would always relax into the dimer geometry. Considering the trimer and the quadrimer, we see that the former tends to the linear chain while the latter tends to the dimer chain. As a result, a detailed analysis of the curves (not reported here) shows that the trimer curve crosses the dimer curve somewhere between $d = 2.92$ Å ($\varepsilon = 0.14$) and $d = 2.95$ Å ($\varepsilon = 0.15$).

In the lower panel of Fig. 2, we see that the tension on the linear chain under uniaxial tension reaches a maximum value of 2.4 nN (1.528 eV/Å) when $\varepsilon_{xx} = 0.184$. This value is in agreement with the recent experimental results of Ref. [8] in which a tensile force of 1.6 ± 0.7 nN was needed to observe the one-dimensional arrays of single gold atoms. Our value is also in agreement with previous DFT-LDA results: 2.2 nN [12], 2.5 nN [14], and 2.4 nN [16]. It is higher than the DFT-GGA value (1.9 nN) reported in Ref. [16], which agrees with the older experimental results 1.5 ± 0.3 nN of Ref. [4].

3.2. Phonons and stability

We now turn to the study of the phonon bandstructures. We start with the linear chain studying the effect of strain, as illustrated in Fig. 4. This figure calls for a series of comments.

Globally, it can be described as follows:

1. for $\varepsilon = 0.09$ (yellow curve), both the transverse and longitudinal modes seem to be stable (the frequencies are positive everywhere);
2. for $\varepsilon < 0.09$ (from orange to red curves), the longitudinal mode is stable whereas the transverse mode is unstable;
3. for $\varepsilon > 0.09$ (from green to blue curves), it is the reverse.

But, as already mentioned, we must pay attention to the possible presence of both Kohn anomalies [46] and Peierls instabilities [47].

For instance, for the longitudinal mode, these induce either an abrupt change (Peierls instability) or a dip (Kohn anomaly) in the bandstructure close to the X point. As a result, focusing on a case for which there is a Peierls instability (e.g. for $\varepsilon = 0.09$), if we apply the

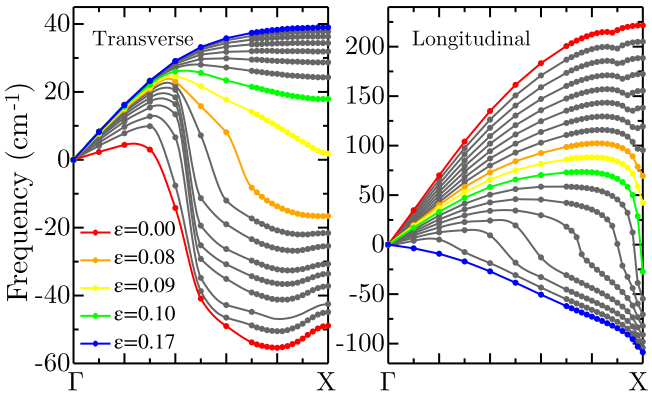

Fig. 4. Phonon dispersion curves of the linear chain as a function of the strain. ϵ = 0.00, 0.07, 0.08, 0.09, 0.17 are represented in red, orange, yellow, green, and blue; the intermediate values of strain being in grey. The left (right) panel shows the transverse (longitudinal) mode.

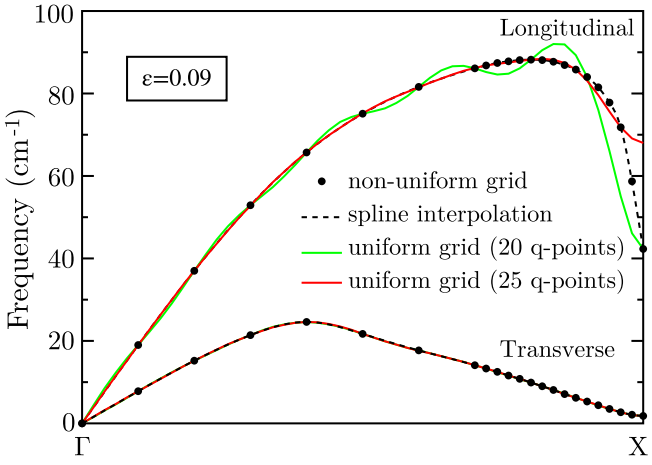

Fig. 5. Phonon bandstructure of the linear chain at ε = 0.09. Explicit calculations (black circles) are compared with different interpolation schemes. The green and red curves are the results obtained using the usual interpolation scheme of the interatomic force constants calculated on a uniform with 20 and 25 q-points, respectively. The first grid explicitly includes the X point, whereas the second does not. The black dashed curve is simply a spline interpolation of the calculations on a non-uniform grid.

usual interpolation scheme of the dynamical matrices (using Fourier transform) for the longitudinal frequencies, we either obtain a smooth curve with an overestimated value at X when the X point is not among the q-point of the uniform grid chosen for the explicit calculations, or a curve oscillating but going to the correct value at X if the X point is among them. This is illustrated in the Fig. 5 for ε = 0.09.

The black circles are the explicit calculations (on a non-uniform grid). The green and red curves are the results obtained using the usual interpolation scheme of the interatomic force constants. The green (red) curve is the result of the interpolation based on calculations on a uniform grid with 20 (25) q-points including (not including) the X point. Increasing the number of q-points in the uniform grid will obviously lead to the same result (either the oscillations reduce or the frequency at the X point converges towards the correct value). However, the number of q-points needs to be very high to get rid of both problems (for instance, we found that there are still oscillations with 50 q-points). In order to overcome these problems, we work with a non-uniform grid (with more q-points in the region where there is an abrupt change) and we interpolate using splines. The resulting phonon bandstructure is the black dashed line in Fig. 5. For the transverse mode, all the schemes lead to the same results since there is no Peierls instability at X.

A second issue with the Peierls instabilities and the Kohn anomalies

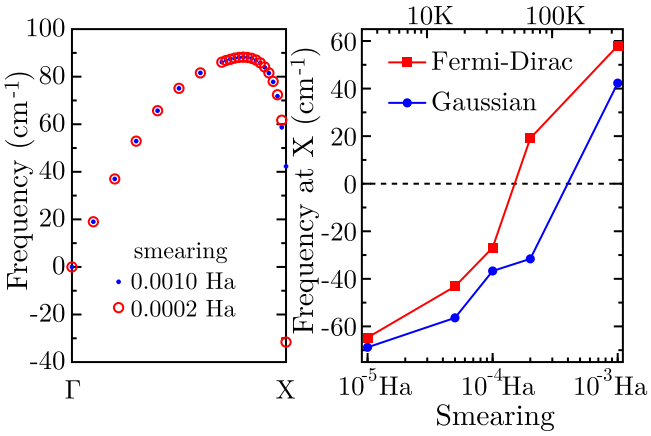

Fig. 6. Effect of the smearing on the Peierls instability for the longitudinal mode of the linear chain at ε = 0.09. In the left panel, the phonon dispersion curve is illustrated for two different values of the Gaussian smearing: 0.0010 Ha (blue dots) and 0.0002 Ha (red circles). In the right panel, the phonon frequencies at X are reported as functions of the Gaussian (blue curve with circles) or Fermi-Dirac (red curve with squares) smearing. When the smearing is too high, the Peierls instability is hidden.

is the effect of the smearing. As already mentioned, the frequencies are positive everywhere for ε = 0.09 (yellow curve) in Fig. 4, even at the X point. However, it seems that there is a Peierls instability that is hidden by the use of the Gaussian smearing. We check this by reducing the smearing to 0.0002 Ha (while carefully checking the convergence with respect to the k-point sampling). We observe that the major part of the curve is not affected but the frequency becomes negative at X, as illustrated in the left panel of Fig. 6. We further decrease the smearing (still checking the convergence with respect to the k-point mesh, using up to 5000 points) focusing on the frequency at the X point. We find that the frequency seems to converge, but this would have to be checked by further decreasing the smearing (while increasing the density of the k-point mesh).

The smearing also has an effect on the Kohn anomaly that appears for the longitudinal mode close to the X point for $0.00 \leqslant \varepsilon \leqslant 0.08$, but the frequency is much less affected. As the strain increases, the Kohn anomaly moves closer and closer to the X point, turning into a Peierls instability. We compute the corresponding electronic bandstructures. In Fig. 7, we report the evolution of the Fermi wavevector k_F as a function of the distance. We see that it decreases until it reaches 0.250 (for

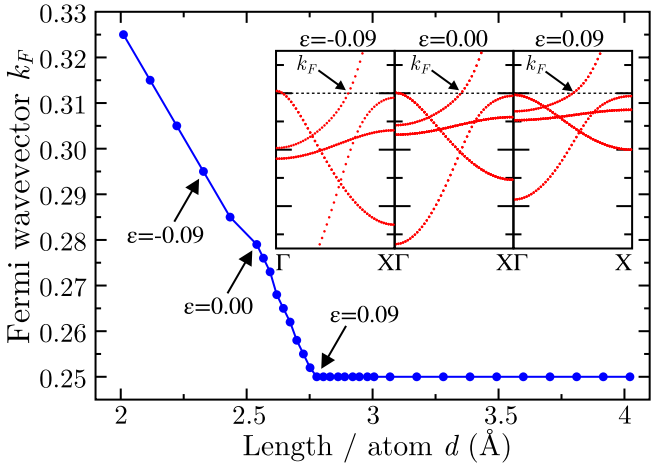

Fig. 7. Evolution of the Fermi wavevector k_F for the linear chain as a function of the length per atom d (expressed in Å). The corresponding electronic bandstructures are illustrated for three different strain values (ε = −0.09, 0.00, and 0.09).

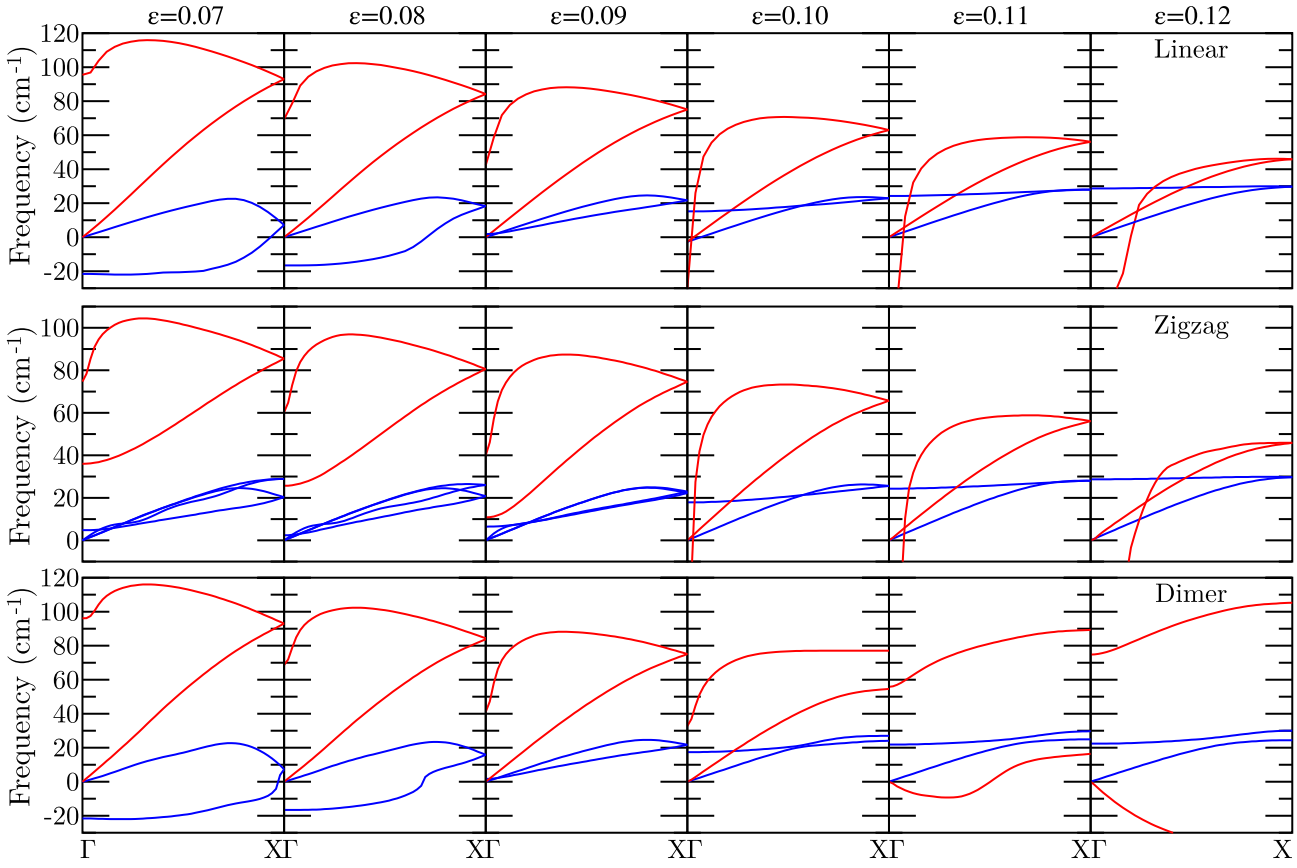

Fig. 8. The phonon dispersion curves of the zigzag and dimer chains compared to those obtained by folding the Brillouin zone for the linear chain. The transverse and longitudinal modes are represented in blue and red, respectively.

$\varepsilon = 0.09$) meaning that $2k_F$ tends to X. The decrease is basically linear though there is a change in the slope at $\varepsilon = 0.00$. This is probably due to the fact that for $\varepsilon < 0.00$ another band also crosses the Fermi level at Γ (hence, it is not fully occupied). From $\varepsilon = 0.00$ on, the maximum of that band is below the Fermi level (the band is fully occupied). Note that close to X, another band approaches the Fermi level but it never crosses it (hence, it is always fully occupied).

Based on the discussion above, there does not seem to be a range of strain for which the linear chain is stable. This in contradiction with one of the main conclusions of Ref. [14]. The smearing that they used was probably too high, hence hiding the Peierls instability.

Finally, we turn to the computation of the phonon bandstructures for the zigzag and dimer chains. Here, there may be a Kohn anomaly at Γ point for both the zigzag and dimer chains. Indeed, due to the zone folding (related to the doubling of the unit cell), the Γ point in these chains is equivalent to the X point in the linear chain (where a Peierls instability could appear). This is causing the oscillations of the highest frequency mode when interpolating using the usual scheme. So, we use a non-uniform mesh of q-points and a spline interpolation, see Fig. 8.

For low strain ($\varepsilon < 0.09$), one of the transverse modes of the dimer chain is unstable at Γ. In contrast, the zigzag chain seems to be stable: the phonon frequencies are positive everywhere from Γ to X. For high strain ($\varepsilon > 0.09$), the zigzag chain is almost linear due to the stretching. Hence, it has an unstable mode (the longitudinal one) at Γ. The dimer chain is stable for $\varepsilon = 0.10$, but it is unstable for higher strain. For $\varepsilon = 0.11$, the biggest instability appears in the longitudinal mode close to Γ. For $\varepsilon = 0.12$, the biggest instability is at X and it is also a longitudinal mode (meaning that the unit cell should be double to allow for a quadrimer to form).

For $\varepsilon = 0.09$, both the dimer and zigzag chain seem to be stable. In fact, the geometries are not very different. In the dimer, the bond length alternation (BLA $= \frac{d_2 - d_1}{d}$) is very small (less than 1%); while in the zigzag chain α is almost 180°. However, as already mentioned, the precise situation at the Γ point must be investigated more carefully: the instability present at the X point in the linear chain could be hidden by the use of the Gaussian smearing of 0.0010 Ha. When reducing the smearing to 0.0002 Ha (while carefully checking the convergence with respect to the k-point sampling), we find that the longitudinal frequency becomes negative at Γ. This indicates that none of these two structures is actually stable. As illustrated in Fig. 9, the equilibrium geometry is a zigzag chain with two different bonds s_1 and s_2, the optimum bond length alternation (BLA $= \frac{s_2 - s_1}{d}$) being very small though (less than 1%).

Following this finding we also investigate more carefully the zigzag chain for $\varepsilon = 0.08$. We find that, when reducing the smearing to 0.0002 Ha, the longitudinal frequency remains positive at Γ. So, for $\varepsilon < 0.09$, the zigzag chain is indeed the optimum geometry.

4. Summary

In this paper, we have investigated monatomic chains of gold using both density functional theory and density functional perturbation theory. Different possible structures (linear, zigzag, dimer, trimer and quadrimer) have been considered for the chains focusing on both their geometry and their energetics as a function of the strain. Then, their stability has been investigated very thoroughly by computing their phonon spectra. We have observed that the linear chain is unstable whatever the strain in contrast with the findings of Ribeiro and Cohen. For low strain ($\varepsilon < 0.09$), the stable geometry was found to be the zigzag chain. For higher strain ($\varepsilon > 0.09$), we observed that the chains with two or more gold atoms are more stable (the trimer and quadrimer chains being even more energetically favorable than the dimer). At the

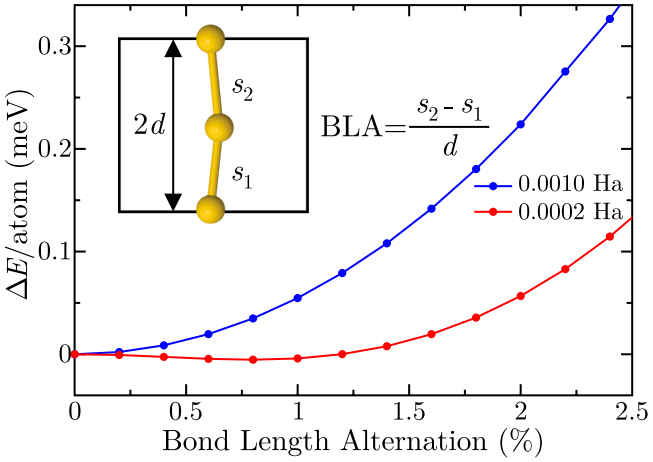

Fig. 9. Effect of the smearing on the instability of the longitudinal mode at Γ for the zigzag chain at $\varepsilon = 0.09$. The cohesive energy per atom as a function of the bond length alternation (BLA) is reported for two different values of the Gaussian smearing: 0.0010 Ha (blue) and 0.0002 Ha (red). The symmetric zigzag chain is chosen as the reference: its cohesive energy is set to zero.

limit between these two regimes ($\varepsilon = 0.09$), we found that the most stable structure is an asymmetric zigzag chain.

CRediT authorship contribution statement

Lianhua He: Investigation, Formal analysis, Writing - original draft, Writing - review & editing, Supervision. **Fang Liu:** Investigation, Formal analysis, Writing - original draft, Writing - review & editing. **Ju Li:** Conceptualization, Investigation, Formal analysis, Writing - review & editing, Funding acquisition. **Gian-Marco Rignanese:** Conceptualization, Investigation, Formal analysis, Writing - original draft, Writing - review & editing, Supervision, Funding acquisition. **Aihui Zhou:** Conceptualization, Investigation, Formal analysis, Resources, Writing - review & editing, Supervision, Funding acquisition.

Acknowledgments

L.H. and F.L. are grateful to the National Science Foundation of China for financial support (grant 11771467). J.L. acknowledges the support by the Skoltech Next Generation Program 2016-7/NGP (a Skoltech-MIT joint project). G.-M.R. is indebted to the Fonds de la Recherche Scientifique-FNRS Belgium for its financial support. A.Z. acknowledges support from the National Science Foundation of China under grants 91730302 and 11671389, and the Key Research Program of Frontier Sciences of the Chinese Academy of Sciences under grant QYZDJ-SSW-SYS010. The calculations were performed on LSSC-II and LSSC-III at the State Key Laboratory of Scientific and Engineering Computing, Chinese Academy of Sciences and Shenteng7000 at the Supercomputing Center, Computer Network Information Center, Chinese Academy of Sciences.

References

[1] H. Ohnishi, Y. Kondo, K. Takayanagi, Quantized conductance through individual rows of suspended gold atoms, Nature 395 (1998) 780–783, https://doi.org/10.1038/27399.
[2] A.I. Yanson, G. Rubio-Bollinger, H.E. van den Brom, N. Agraït, J.M. van Ruitenbeek, Formation and manipulation of a metallic wire of single gold atoms, Nature 395 (1998) 783–785, https://doi.org/10.1038/27405.
[3] E. Tosatti, S. Prestipino, S. Kostlmeier, A. Dal Corso, F. Di Tolla, String tension and stability of magic tip-suspended nanowires, Science 291 (2001) 288, https://doi.org/10.1126/science.291.5502.288.
[4] G. Rubio-Bollinger, S.R. Bahn, N. Agraït, K.W. Jacobsen, S. Vieira, Mechanical properties and formation mechanisms of a wire of single gold atoms, Phys. Rev. Lett. 87 (2001) 026101, , https://doi.org/10.1103/PhysRevLett. 87.026101.
[5] S.B. Legoas, D.S. Galvão, V. Rodrigues, D. Ugarte, Origin of anomalously long interatomic distances in suspended gold chains, Phys. Rev. Lett. 88 (2002) 076105, , https://doi.org/10.1103/PhysRevLett. 88.076105.
[6] C. Untiedt, A.I. Yanson, R. Grande, G. Rubio-Bollinger, N. Agraït, S. Vieira, J.M. van Ruitenbeek, Calibration of the length of a chain of single gold atoms, Phys. Rev. B 66 (2002) 085418, , https://doi.org/10.1103/PhysRevB.66.085418.
[7] S. Olliges, P.A. Gruber, V. Auzelyte, Y. Ekinci, H.H. Solak, R. Spolenak, Tensile strength of gold nanointerconnects without the influence of strain gradients, Acta Mater. 55 (2007) 5201–5210, https://doi.org/10.1016/j.actamat.2007.05.039.
[8] T. Kizuka, Atomic configuration and mechanical and electrical properties of stable gold wires of single-atom width, Phys. Rev. B 77 (2008) 155401, , https://doi.org/10.1103/PhysRevB.77.155401.
[9] D.T. Smith, J.R. Pratt, F. Tavazza, L.E. Levine, A.M. Chaka, An ultrastable platform for the study of single-atom chains, J. Appl. Phys. 107 (2010) 084307, , https://doi.org/10.1063/1.3369584.
[10] R. Dou, B. Derby, Deformation mechanisms in gold nanowires and nanoporous gold, Philos. Mag. 91 (2011) 1070–1083, https://doi.org/10.1080/14786435.2010.481271.
[11] J. Aulbach, J. Schäfer, S.C. Erwin, S. Meyer, C. Loho, J. Settelein, R. Claessen, Evidence for long-range spin order instead of a Peierls transition in Si(553)-Au chains, Phys. Rev. Lett. 111 (2013) 137203, , https://doi.org/10.1103/PhysRevLett. 111.137203.
[12] D. Sánchez-Portal, E. Artacho, J. Junquera, P. Ordejón, A. García, J.M. Soler, Stiff monatomic gold wires with a spinning zigzag geometry, Phys. Rev. Lett. 83 (1999) 3884, https://doi.org/10.1103/PhysRevLett. 83.3884.
[13] D. Sánchez-Portal, E. Artacho, J. Junquera, A. García, J.M. Soler, Zigzag equilibrium structure in monatomic wires, Surf. Sci. 482–485 (2001) 1261–1265, https://doi.org/10.1016/S0039-6028(01)00875-5.
[14] F.J. Ribeiro, M.L. Cohen, Ab initio pseudopotential calculation of infinite monatomic chains of Au, Al, Ag, Pd, Rh, and Ru, Phys. Rev. B 68 (2003) 035423, , https://doi.org/10.1103/PhysRevB.68.035423.
[15] F. Picaud, A. Dal Corso, E. Tosatti, Phonons softening in tip-stretched monatomic nanowires, Surf. Sci. 532–535 (2003) 544–548, https://doi.org/10.1016/S0039-6028(03)00231-0.
[16] E.Z. da Silva, F.D. Novaes, A.J.R. da Silva, A. Fazzio, Theoretical study of the formation, evolution, and breaking of gold nanowires, Phys. Rev. B 69 (2004) 115411, , https://doi.org/10.1103/PhysRevB.69.115411.
[17] D. Çakír, O. Gülseren, Effect of impurities on the mechanical and electronic properties of Au, Ag, and Cu monatomic chain nanowires, Phys. Rev. B 84 (2011) 085450, , https://doi.org/10.1103/PhysRevB.84.085450.
[18] M. Okamoto, K. Takayanagi, Structure and conductance of a gold atomic chain, Phys. Rev. B 60 (1999) 7808, https://doi.org/10.1103/PhysRevB.60.7808.
[19] L. De Maria, M. Springborg, Electronic structure and dimerization of a single monatomic gold wire, Chem. Phys. Lett. 323 (2000) 293–299, https://doi.org/10.1016/S0009-2614(00)00541-8.
[20] N.V. Skorodumova, S.I. Simak, Spatial configurations of monoatomic gold chains, Comput. Mater. Sci 17 (2000) 178, https://doi.org/10.1016/S0927-0256(00)00019-7.
[21] J. Diao, K. Gall, M.L. Dunn, J.A. Zimmerman, Atomistic simulations of the yielding of gold nanowires, Acta Mater. 54 (2006) 643–653, https://doi.org/10.1016/j.actamat.2005.10.008.
[22] E. Fabiano, L.A. Constantin, F.D. Sala, Exchange-correlation generalized gradient approximation for gold nanostructures, J. Chem. Phys. 134 (2011) 194112, , https://doi.org/10.1063/1.3587054.
[23] M.R. Sørensen, M. Brandbyge, K.W. Jacobsen, Mechanical deformation of atomic-scale metallic contacts: Structure and mechanisms, Phys. Rev. B 57 (1998) 3283–3294, https://doi.org/10.1103/PhysRevB.57.3283.
[24] H.S. Park, J.A. Zimmerman, Modeling inelasticity and failure in gold nanowires, Phys. Rev. B 72 (2005) 054106, , https://doi.org/10.1103/PhysRevB.72.054106.
[25] Q. Pu, Y. Leng, L. Tsetseris, H.S. Park, S.T. Pantelides, P.T. Cummings, Molecular dynamics simulations of stretched gold nanowires: the relative utility of different semiempirical potentials, J. Chem. Phys. 126 (2007) 144707, , https://doi.org/10.1063/1.2717162.
[26] L. Ke, T. Kotani, M. van Schilfgaarde, P.A. Bennett, Breakdown of a gold nanowire between electrodes, Nanotechnology 18 (2007) 424002, , https://doi.org/10.1088/0957-4484/18/42/424002.
[27] E.Y. Zarechnaya, N.V. Skorodumova, S.I. Simak, B. Johansson, E.I. Isaev, Theoretical study of linear monoatomic nanowires, dimer and bulk of Cu, Ag, Au, Ni, Pd and Pt, Comp. Mater. Sci. 43 (2008) 522–530, https://doi.org/10.1016/j.commatsci.2007.12.018.
[28] Y.-H. Wen, Q. Wang, K.M. Liew, Z.-Z. Zhu, Compressive mechanical behavior of Au nanowires, Phys. Lett. A 374 (2010) 2949–2952, https://doi.org/10.1016/j.physleta.2010.05.015.
[29] F. Tavazza, L.E. Levine, A.M. Chaka, Structural changes during the formation of gold single-atom chains: stability criteria and electronic structure, Phys. Rev. B 81 (2010) 235424, , https://doi.org/10.1103/PhysRevB.81.235424.
[30] A. Kumar, A. Kumar, P.K. Ahluwalia, Ab initio study of structural, electronic and dielectric properties of free standing ultrathin nanowires of noble metals, Physica E 46 (2012) 259–269, https://doi.org/10.1016/j.physe.2012.09.032.
[31] S. Bansal, R. Priyanka, K. Bhandari, Dharamvir, Monatomic gold nanochains and their encapsulation in au60au9 tubular structure, International Conference on Advanced Nanomaterials & Emerging Engineering Technologies, 2013, pp. 305–308, , https://doi.org/10.1109/ICANMEET.2013.6609298.
[32] P. Alves da Silva Autreto, D.S. Galvao, E. Artacho, Species fractionation in atomic chains from mechanically stretched alloys, J. Phys.: Condens. Matter 26 (2014) 435304, , https://doi.org/10.1088/0953-8984/26/43/435304.
[33] A. Kumar, P.K. Ahluwalia, Transport properties of pristine and alloyed free standing

ultrathin nanowires of noble metals, J. Alloys Compd. 615 (2014) 194–203, https://doi.org/10.1016/j.jallcom.2014.05.210.
[34] F. Wang, Y. Dai, J. Zhao, Q. Li, Uniaxial tension-induced fracture in gold nanowires with the dependence on size and atomic vacancies, Phys. Chem. Chem. Phys. 16 (2014) 24716, https://doi.org/10.1039/C4CP03556A.
[35] C. Zhu, J.-X. Liang, G. Wei, Theoretical investigation of an ultrastable one dimensional infinite monatomic mixed valence gold wire with excellent electronic properties, Phys. Chem. Chem. Phys. 18 (2016) 12338, https://doi.org/10.1039/C6CP00787B.
[36] S. Sanna, T. Lichtenstein, Z. Mamiyev, C. Tegenkamp, H. Pfnür, How one-dimensional are atomic gold chains on a substrate? J. Phys. Chem. C 122 (2018) 25580–25588, https://doi.org/10.1021/acs.jpcc.8b08600.
[37] J.-X. Liang, Y.X. Wu, H.F. Deng, C.L. Long, C. Zhu, Theoretical investigation on the electronic structure of one dimensional infinite monatomic gold wire: insights into conducting properties, RSC Adv. 9 (2019) 1373–1377, https://doi.org/10.1039/C8RA08286C.
[38] W. Kohn, L.J. Sham, Self-consistent equations including exchange and correlation effects, Phys. Rev. 140 (1965) A1133, https://doi.org/10.1103/PhysRev. 140.A1133.
[39] S. Baroni, P. Giannozzi, A. Testa, Green's-function approach to linear response in solids, Phys. Rev. Lett. 58 (1987) 1861, https://doi.org/10.1103/PhysRevLett. 58.1861.
[40] X. Gonze, J.-P. Vigneron, Density-functional approach to nonlinear-response coefficients of solids, Phys. Rev. B 39 (1989) 13120, https://doi.org/10.1103/PhysRevB.39.13120.
[41] X. Gonze, F. Jollet, F.A. Araujo, D. Adams, B. Amadon, T. Applencourt, C. Audouze, J.-M. Beuken, J. Bieder, A. Bokhanchuk, E. Bousquet, F. Bruneval, D. Caliste, M. Côté, F. Dahm, F.D. Pieve, M. Delaveau, M.D. Gennaro, B. Dorado, C. Espejo, G. Geneste, L. Genovese, A. Gerossier, M. Giantomassi, Y. Gillet, D. Hamann, L. He, G. Jomard, J.L. Janssen, S.L. Roux, A. Levitt, A. Lherbier, F. Liu, I. Lukačevič, A. Martin, C. Martins, M. Oliveira, S. Poncé, Y. Pouillon, T. Rangel, G.-M. Rignanese, A. Romero, B. Rousseau, O. Rubel, A. Shukri, M. Stankovski, M. Torrent, M.V. Setten, B.V. Troeye, M. Verstraete, D. Waroquiers, J. Wiktor, B. Xu, A. Zhou, J. Zwanziger, Recent developments in the ABINIT software package, Comput. Phys. Commun. 205 (2016) 106–131, https://doi.org/10.1016/j.cpc.2016.04.003.
[42] L. He, F. Liu, G. Hautier, M.J.T. Oliveira, M.A.L. Marques, F.D. Vila, J.J. Rehr, G.M. Rignanese, A. Zhou, Accuracy of generalized gradient approximation functionals for density-functional perturbation theory calculations, Phys. Rev. B 89 (2014) 064305, , https://doi.org/10.1103/PhysRevB.89.064305.
[43] J.L. Martins, N. Troullier, S.-H. Wei, Pseudopotential plane-wave calculations for zns, Phys. Rev. B 43 (1991) 2213–2217, https://doi.org/10.1103/PhysRevB.43.2213.
[44] M. Methfessel, A.T. Paxton, High-precision sampling for Brillouin-zone integration in metals, Phys. Rev. B 40 (1989) 3616, https://doi.org/10.1103/PhysRevB.40.3616.
[45] N. Mermin, Thermal properties of the inhomogeneous electron gas, Phys. Rev. 137 (1965) A1441, https://doi.org/10.1103/PhysRev. 137.A1441.
[46] W. Kohn, Image of the Fermi surface in the vibration spectrum of a metal, Phys. Rev. Lett. 2 (1959) 393, https://doi.org/10.1103/PhysRevLett. 2.393.
[47] R.E. Peierls, Quantum Theory of Solids, Clarendon Press, Oxford, 1955.